Nuclear Instruments and Methods in Physics Research A247 (1986) 445–452
North-Holland, Amsterdam

A NOVEL TYPE OF PARALLEL PLATE CHAMBER WITH RESISTIVE GERMANIUM ANODE AND A TWO-DIMENSIONAL READOUT

R. BELLAZZINI, C. BETTI, A. BREZ, E. CARBONI, M.M. MASSAI and M.R. TORQUATI

Dipartimento di Fisica dell'Università di Pisa and INFN, Sezione di Pisa, Via Livornese, 582/A San Piero a Grado, 56010 Pisa, Italy

Received 30 July 1985 and in revised form 4 December 1985

A parallel plate counter with a resistive anode and a two-dimensional readout is presented. The anode is made of a thin germanium layer with a sheet resistivity $\geqslant 1$ MΩ/square and the cathode is made of aluminized mylar 5 μm thick. The anode is transparent to the fast impulse due to the collection of the multiplication electrons. A chessboard of "pads" placed behind the anode plane is used to obtain the positional information. The detector and the readout system are physically and logically separated. An overall spatial resolution of 70 μm (rms) for both coordinates has been measured.

1. Introduction

In many low or high energy physics experiments it is often necessary or desirable to measure with high resolution the three spatial coordinates of the impact point of an ionizing particle with a single detector. Usually this cannot be achieved with wire chambers because the resolution in the direction orthogonal to the wires is severely limited by the wire pitch. A solution to this problem could be found by using a continuous and homogeneous detector, like a parallel plate counter, but still preserving the positional sensitivity typical of discrete structures.

Parallel plate counters have been used for several years in nuclear physics as detectors of highly ionizing particles [1–3]. More recently [4] they have been proposed also, as a possible alternative to wire chambers, as detectors of low ionization particles. Their main features are: (1) very good time resolution, (2) high data rate capability, (3) total insensitivity to radiation damage. Their major drawback is the null or poor position sensitivity and the low detection efficiency for minimum ionizing particles when operated at low gas pressure. To overcome these problems we have designed, built and tested a new type of parallel plate avalanche chamber. This detector has a resistive anode and a high resolution two-dimensional readout and works at atmospheric or higher pressure. Because of its high resistivity the anode is transparent to the fast impulse generated by the avalanche electrons. Behind the anode plane a chessboard of "pads" collects this fast impulse and it is used to obtain the position sensitivity.

In this paper the principle of operation and the preliminary results of laboratory tests of this detector are presented.

2. Principle of operation of the detector

2.1. Gas gain

A parallel plate chamber (PPC) consists of two continuous electrodes mounted parallel to each other (see fig. 1). When a potential difference is applied between close electrodes, a uniform, intense electric field is established inside the detector volume. Ionization electrons delivered by a traversing particle start to multiply until they are collected by the anode. In the case of point ionization the number of secondary electrons is given by:

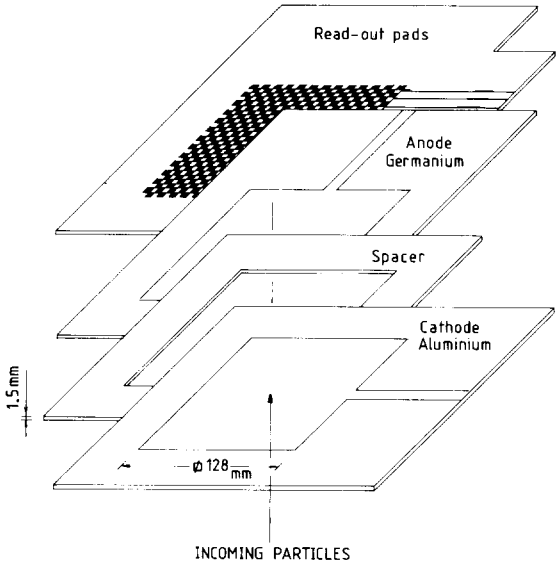

Fig. 1. Perspective view of the detector assembly.

$$n = n_0 \, e^{\alpha d}, \tag{1}$$

with n_0 the number of primary electrons, d the drift length and α the first Townsend coefficient.

In the case of extended (track) ionization the number of secondary electrons is given, assuming a uniform specific ionization along the track, by

$$n = \int_0^d \frac{n_0}{d} e^{\alpha x} \, dx. \tag{2}$$

Ionization collisions close to the cathode give a greater contribution to the total signal than those close to the anode. A gas gain up to 10^4–10^5 can be obtained. This signal has an amplitude of a few hundreds of μV and consists of two parts:

1) a fast rising component due to the collection of the electrons,
2) a slowly rising component due to the positive ions with their much lower drift velocity.

2.2. The resistive anode

If the electrode plates are both made of a conducting material a voltage pulse due to the collection of the drifting charges can be observed in a external circuit connected to one of the electrodes. However, because the whole electrode plane moves to the new potential no positional information can be obtained from this signal.

The situation is completely different if one or both of the electrodes are made of a semiconducting material with a sufficiently high sheet resistivity. In this case we can consider the electrode as a two-dimensional array of resistances [5]. If an array (one- or two-dimensional) of capacitances is placed behind the resistive plane a "short-circuit" to ground is established for impulsive current (see fig. 2). We can say that the resistive plane acts as a conductor for dc currents, so that it can be charged to a suitable potential, while it acts as a dielectric for very short currents so that it is transparent to the corresponding impulses. The positional information can be obtained from the distribution of the charge collected on the external capacitances.

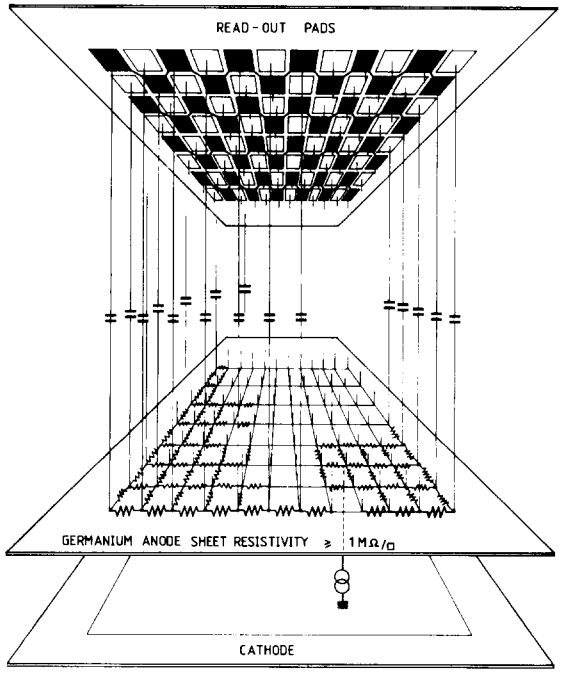

Fig. 2. Electric representation of the anode transparency concept.

3. Detector design and construction

The material we chose for the construction of the resistive electrode is germanium. Germanium has a bulk resistivity of 60 Ω cm. A 1–0.1 μm thick deposit obtained via vacuum evaporation results in a sheet resistivity in the range 0.5–50 MΩ/square which is high enough to ensure the full transparency of the fast component of the signals coming from the detector. Further advantages of the vacuum evaporation are the high uniformity of the deposit ($\pm 1\%$) and the easily controllable value of the resistivity which is a function only of the thickness of the deposit. The high uniformity of the sheet resistivity allows one to work at values of resistivity close to the one corresponding to the full transparency threshold, thus reducing the rate limitations of the device (see sect. 6). As a support of the germanium deposit we used machined epoxy planes or polished glass (see fig. 3). The cathode is made of aluminized mylar 5 μm thick. This light material was selected to have an entrance window for short range particles such

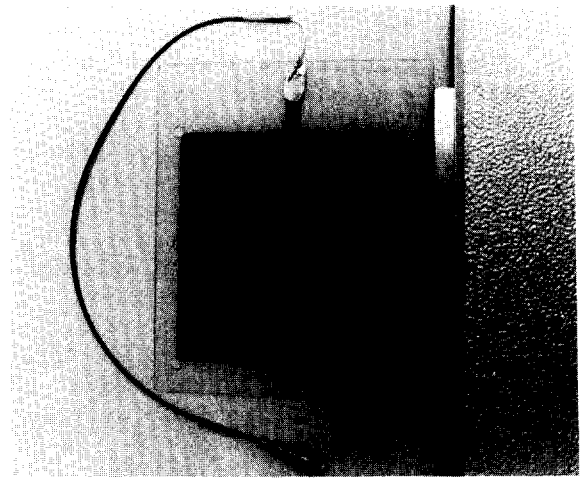

Fig. 3. The resistive anode obtained using a germanium deposit on a glass plate.

as low energy X- or β^--rays. The gap between the anode and the cathode was obtained with spacers made of epoxy having a thickness in the range of 1–3 mm. Special care was taken during the machining of the epoxy planes to ensure good planarity of the anode plate and good uniformity of the spacer thickness (± 0.005 mm tolerance). Parallel alignment of the electrode plates implies that the mylar foil is without any wrinkles and well stretched. In this way it can act also as a restoring force againgst the electrostatic attraction, thus minimizing the sagitta in the middle of the chamber. In order to obtain a well stretched foil the following technique was used for the construction of the cathode plane. An aluminized mylar foil was glued onto a metal ring of 40 cm diameter and 6 kg weight. The foil thus fixed on the ring was brought down over a lucite disc of 30 cm diameter. The mylar foil was then stretched uniformly into all directions by the weight of the ring. To further increase the stretching of the foil the air volume under the foil was evacuated down to 0.1 atm using a water pump. The epoxy frame of the cathode was divided into two parts by a 1 mm thick groove. After having coated the external part with a thin film of glue, the frame was brought down on the mylar foil and the glue allowed to harden. The groove collects the excess glue so that no liquid epoxy can flow into the internal side of the frame where the spacer will be stacked.

The detector active area A is 13 cm × 13 cm and the gas filling was argon (90%)–methane (10%). A typical operating voltage when working at normal pressure and with a ^{55}Fe illumination was 3.2 kV corresponding to a uniform electric field of 16.0 kV/cm for a 2 mm gap. The electrostatic force between the anode and cathode plane is $F = \frac{1}{2}\epsilon_0 A(V/d)^2 \simeq 20$ g for $d = 2$ mm, $V = 3.2$ kV and $\epsilon_0 = 8.85 \times 10^{-12}$ F/m. To measure the gap uniformity when the electric field is established we used a holographic technique (see fig. 4). By means of a laser beam ($\lambda = 6030$ Å) we took a hologram of the cathode plane when no potential difference was applied. If we put a hologram of an object in the same place where it

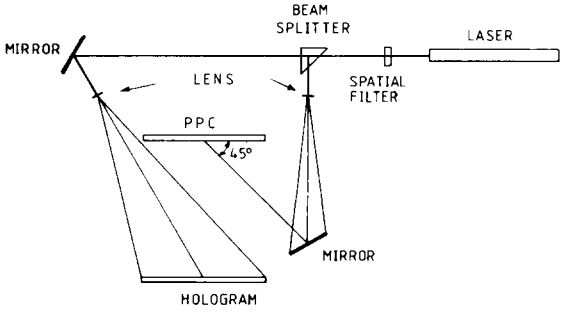

Fig. 4. Scheme of the setup utilized for the holographic measurement of the sagitta.

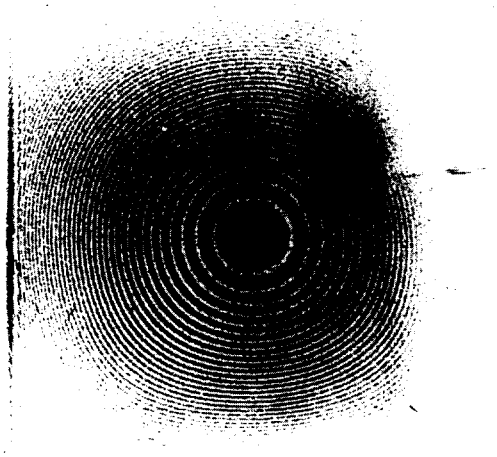

Fig. 5. Typical interference fringes observed when a potential difference is applied.

has been recorded and, after having removed the object, we illluminate the hologram with the same laser beam we reconstruct the light wave which has been diffused by the object during the exposure. If the object is not removed, we observe two waves: the one coming directly from the object and the one reconstructed from the hologram. These two waves are coherent and therefore they can interfere. If the object undergoes some deformations before the second exposure, these will be observed on the final image as interference fringes due to differences in the optical path which equal an integral number of source wavelengths (see fig. 5). The maximum deformation h is, in our case, related to n, the

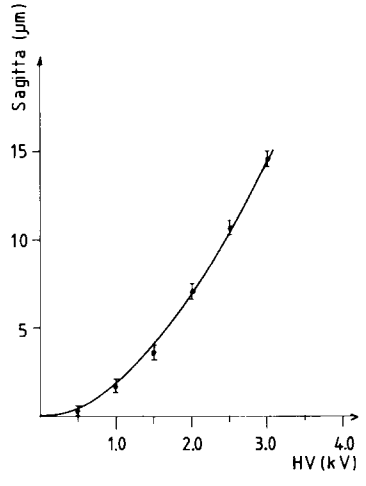

Fig. 6. The dependence of the sagitta on the applied voltage.

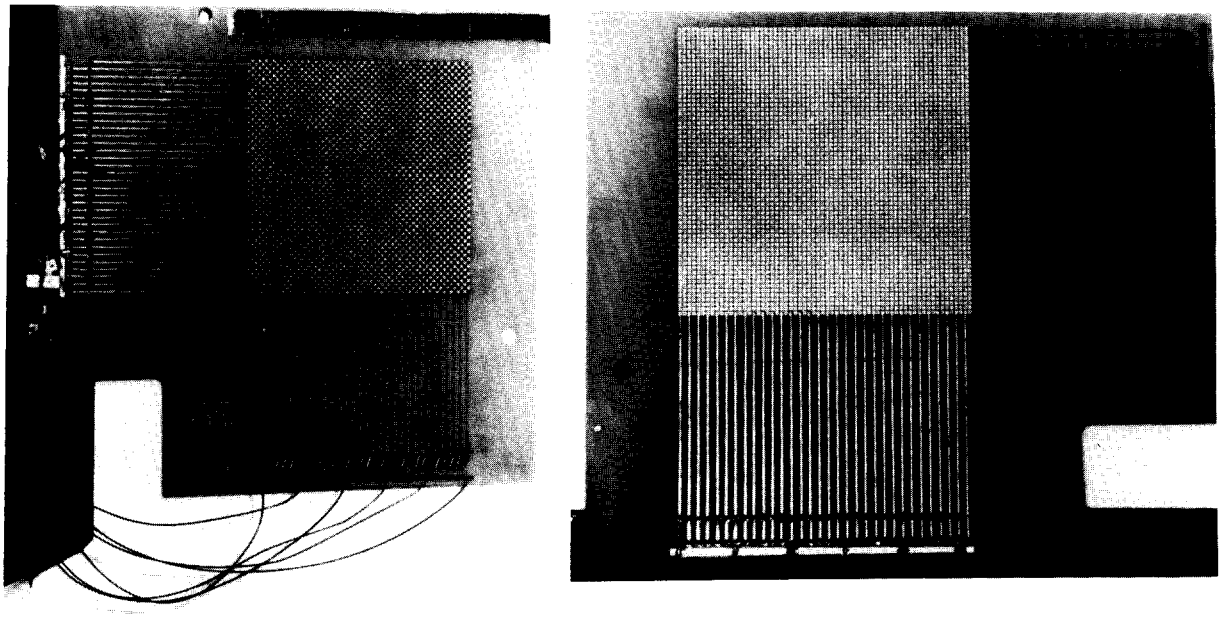

Fig. 7. The two sides of the readout chessboard.

total number of interference fringes by the relation $h = n(\lambda/2)\sin\alpha$, where α is the angle of incidence of the laser light on the object. Fig. 6 shows the dependence of the sagitta on the applied voltage. The maximum sagitta was $\simeq 15$ μm for $d = 2$ mm and $V = 3.0$ kV.

Behind the anode plane a double-sided chessboard of 2 mm $\times$ 2 mm "pads" collects the fast electron impulse and is used to obtain the event position. Half of the pads are zig-zag connected to form rows on one side of the chessboard. Metallized holes of 0.5 mm diameter connect the remaining half of the pads to form collumns on the back of the chess-board (see fig. 7). In this way a two-dimensional readout is obtained looking at the detector from one side only, leaving the front side free as a window for the incoming particles.

The advantages of this setup are:

1) two-dimensional positional information is obtained from a perfectly homogeneous, self-triggering detector;
2) the detector and the readout system are physically and logically separated so that they can be optimized independently;
3) the data rate is subdivided over the whole detector volume;
4) because the cathode is the entrance window and the electrons created close to the cathode have the largest gain, an "electronic collimation" of inclined tracks is obtained;
5) the detector is mechanically very simple and sturdy (no fragile wires etc.).

4. The readout system

The event position is obtained from the measurement of the centroid of the charge distribution on the readout pads. The electronic chain consists of a low noise charge preamplifier [6], a linear amplifier with a 2 μs Gaussian shaping and a peak-sensing ADC for each row and column. For these preliminary measurements a 25 mm $\times$ 25 mm central region was instrumented with 6 channels for each coordinate. The data acquisition is started and gated by the prompt signal obtained from the cathode plane. The distance of the readout plane from the anode plane can be easily adjusted depending on the pitch of the rows and columns. The relative gains of each channel were equalized within 1%. To find the value of the event position we have adopted two different algorithms. The first is the direct calculation of the center of gravity of the measured distribution obtained trough the relation $X = \Sigma_i Q_i / \Sigma_i Q_i$, while the second relies on the shape of the charge distribution [7]. If Q_i is the channel containing the maximum of the charge distribution, we can define $R^+ = Q_{i+1}/Q_i$ and $R^- = Q_{i-1}/Q_i$. Both R^+ and R^- are functions of x, the true event position inside the strip i, i.e. $R^+ \equiv R^+(x)$ and $R^- \equiv R^-(x)$. If the theoretical dependence upon x of $R^+(x)$ and $R^-(x)$ is known from a model of the induction process, then the measured values R^+ and R^- allow a determination of the event position. The electrostatic distribution of the charge induced by a point charge places between the cathode and the readout plane well reproduced the measured distribution

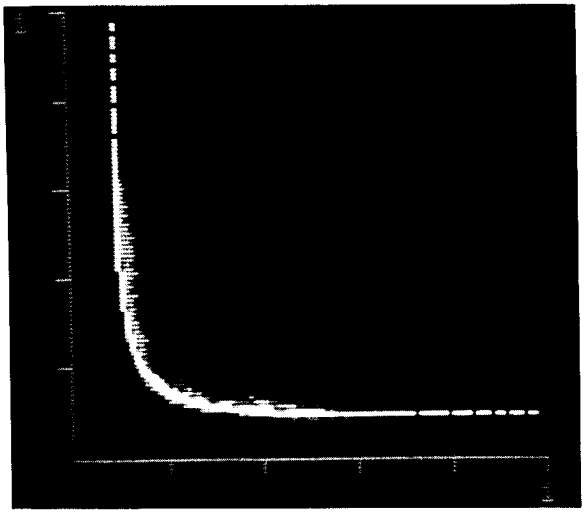

Fig. 8. Scatter plot Q_{i-1}/Q_i vs Q_{i+1}/Q_i with superimposed the theoretical fit (the brighter curve) obtained from the electrostatic model of charge induction.

and was used to obtain the value of the estimator of the true event position [8,9]. Fig. 8 shows the scatter plot of R^- versus R^+ as measured in our chamber with superimposed the theoretical fit obtained from the electrostatic model of the charge induction. The best estimate of the avalanche position is given by the intersection of the theoretical curve with the line connecting the data point and the point (1,1). The two reconstruction algorithms give roughly the same results. The algorithm exploiting the shape of the charge distribution has the additional advantage that, unlike in the center of gravity method, the differential nonlinearity does not depend so strongly on the ratio of the strip pitch to the distance between the anode and the readout plane. For a more detailed discussion of the reconstruction algorithms and their relative merits we refer to a forthcoming paper [10].

5. Results

The results described in this paper refer to the operation of the chamber at standard pressure. The chamber has also been operated for some time at 2 atm absolute pressure without any particular problem.

Fig. 9 shows the typical current signal on the cathode plane when a detector with a 2 mm gap is irradiated with a ^{55}Fe source. The fast electron component and the slow tail due to the collection of the positive ions are apparent. The electroninc amplification was $A = 500$. The height of the plateau in fig. 9 is proportional to the ion current component $i = n_0 \exp(\alpha d)/T$, where T is the duration of the ion collection process (5 μs in this case). Because the preamplifier has an input impedance

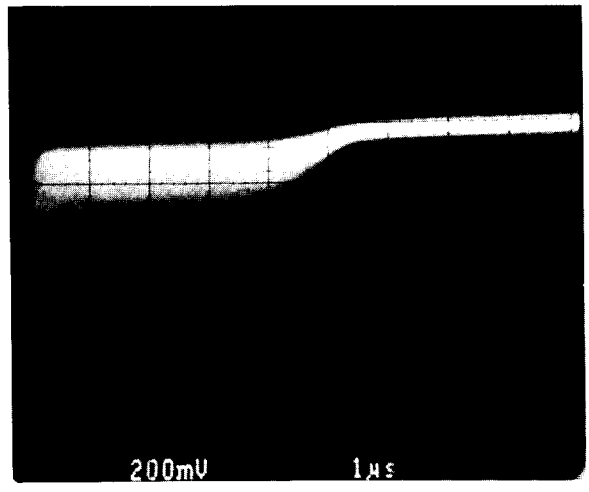

Fig. 9. The typical current signal on the cahode plane when the detector is irradiated with a ^{55}Fe source.

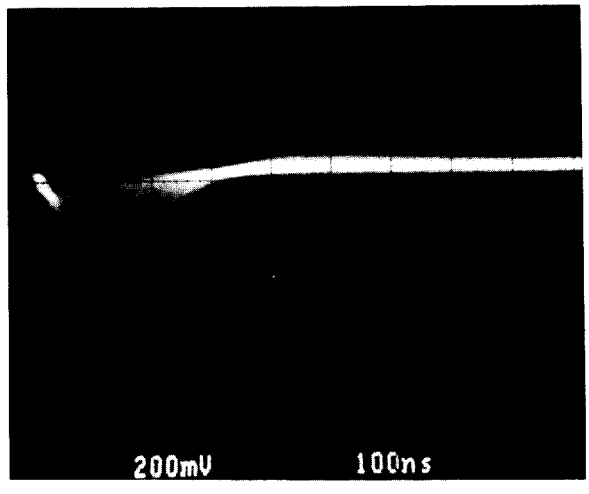

Fig. 10. The electron component of the signal observed after differentiation of the signal of fig. 9.

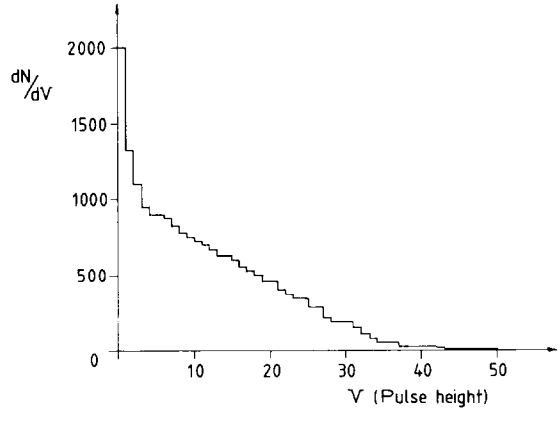

Fig. 11. Pulse height spectrum of the signal of fig. 9.

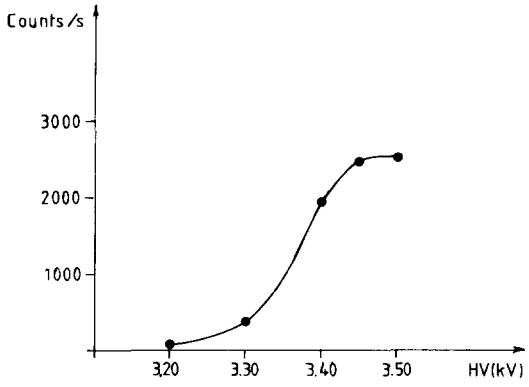

Fig. 12. The dependence of the counting rate on the operating voltage when the chamber is irradiated with a ^{90}Sr source.

$Z = 500\ \Omega$, we can use the result of fig. 9 to estimate the gas gain $G = \exp(\alpha d) = VT/AZn_0e$, where V is the maximum output voltage, n_0 the number of primary electrons created at the cathode ($= 200$ for ^{55}Fe) and e is the electron charge. A gas gain factor $G = 10^5$ can be estimated for $d = 2$ mm. Fig. 10 shows the fast component of the signal after differentiation of the slow component. The differentiation time constant was $\tau = 500$ ns.

Fig. 11 shows the pulse height spectrum of the signal of fig. 9. The spectrum is almost continuous because for each conversion point there is a different gain according to the law $G = \exp(\alpha d)$. Fig. 12 shows the dependence of the counting rate (singles) on the operating voltage

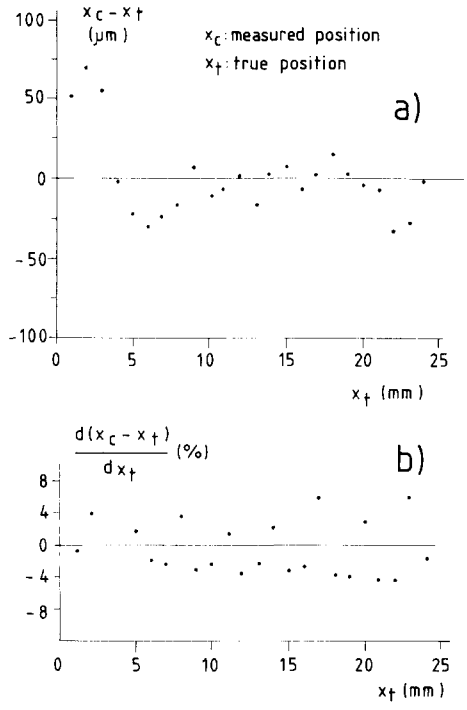

Fig. 14. (a) The integral nonlinearity. (b) The differential nonlinearity.

for a collimated ^{90}Sr source emitting β^--rays with an endpoint energy of 2.27 MeV. The PPC had a 2 mm gap.

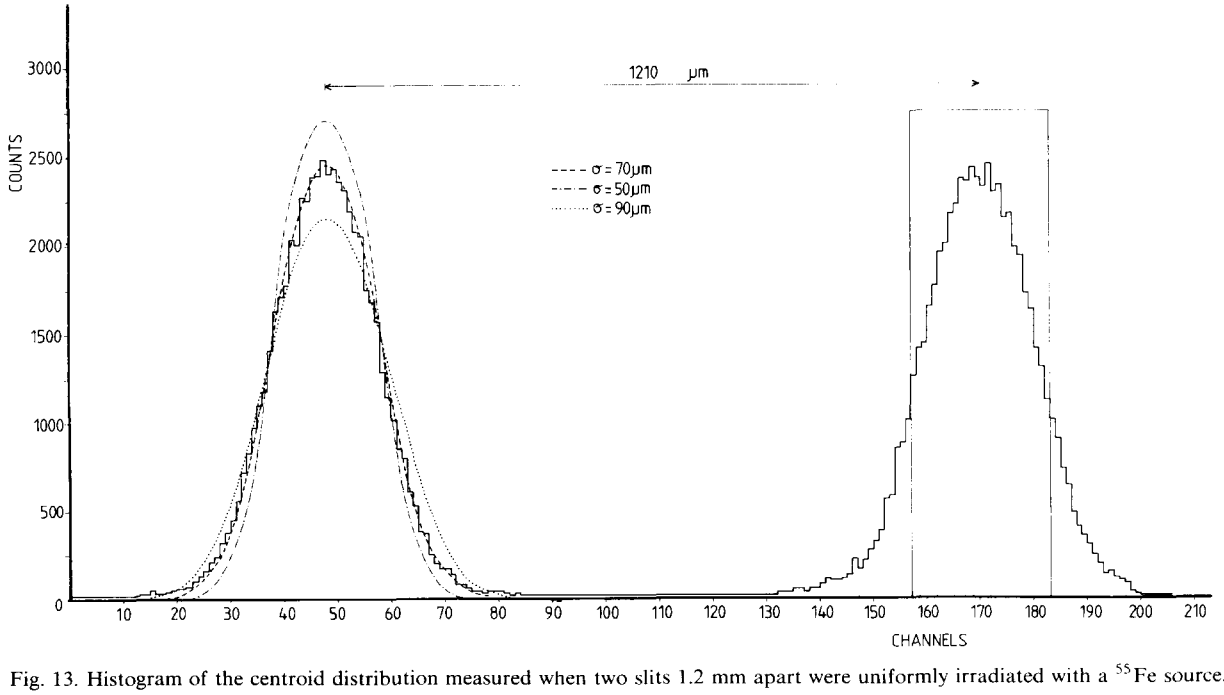

Fig. 13. Histogram of the centroid distribution measured when two slits 1.2 mm apart were uniformly irradiated with a ^{55}Fe source.

The uniformity of response was checked moving a collimated ^{55}Fe source across the detector. The recorded counting rate was constant within $\pm 5\%$. To measure the spatial resolution in one coordinate we have built a resolution phantom constituted of two slits 220 and 255 μm wide, 1.2 mm apart, which were uniformly illuminated with a ^{55}Fe source. Fig. 13 shows the histogram of the centroid distribution as measured with the center of gravity method. The widths (fwhm) of the peaks are ≈ 225 and ≈ 260 μm indicating that the resolution is much better than the slit width. To have a quantitative estimate of the resolution we have used a mathematical model. We have assumed that the histogram of fig. 13 is the result of the convolution product of a square wave with a Gaussian function. The resolution is the width of that Gaussian funcion which , when convoluted with the square wave, gives the best fit to the data of fig. 13. The results of this type of modeling are shown in fig. 13 for three Gaussian functions with a σ of 50, 70 and 90 μm respectively. The best fit is obtained for $\sigma = 70$ μm.

This figure includes all the possible sources of errors. The major contributions arise from the finite range of the primary photoelectrons created by the interaction of the 5.9 keV ^{55}Fe X-rays with argon and from the geometrical misalignment of the slits relative to the readout strips.

The integral and the differential nonlinearity were studied by moving the two slits across the central (instrumented) part of the detector by means of a micrometric screw. The maximum absolute position error and the maximum differential nonlinearity were found to be 70 μm and 4% respectively (see fig. 14). To study the two-dimensional reconstruction capability of the device we have utilized a resolution phantom which is shown in fig. 15 together with the reconstructed image. In this latter case the charge-ratio algorithm was used.

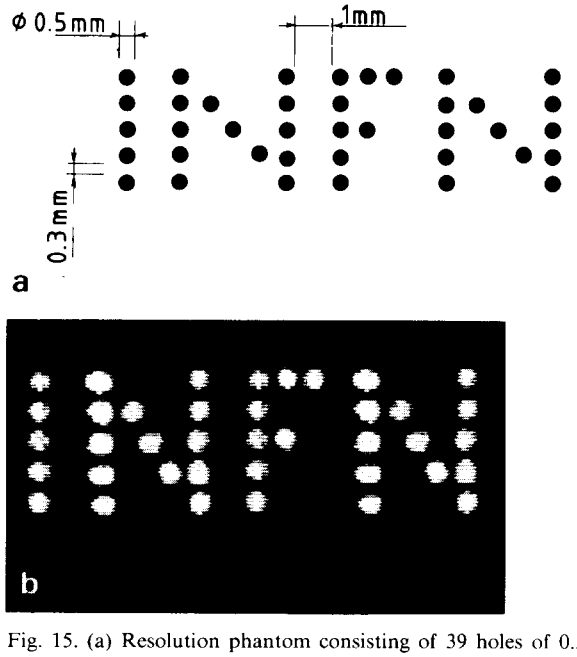

Fig. 15. (a) Resolution phantom consisting of 39 holes of 0.5 mm diameter, 0.3 mm apart arranged to form the word INFN. (b) The reconstructed image (^{55}Fe source).

6. Rate limitations

Resistive plate chambers could suffer from rate problems [5]. If a uniform flux of particles N s^{-1} cm^{-2} interacts with a device of area A a voltage drop $V = I\bar{R}NA$ due to the discharge process will be observed, I being the equivalent dc current due to the detection of one particle per second and $\bar{R}$ the total mean resistance of the anode plate. $\bar{R}$ depends on the shape of the resistive electrode and on the number and shape of the ohmic contacts. In the case of a square anode with two ohmic contacts along two opposite sides, the maximum resistance is found for events interacting in the middle of the chamber and is $R_{max} = \frac{1}{2}R_{\square} \| \frac{1}{2}R_{\square} = \frac{1}{4}R_{\square}$. We can therefore assume $\frac{1}{4}R_{\square}$ as an upper limit for $\bar{R}$.

In our case the situation is favorable because the detector is operated at very low gas gain (10^4–10^5) and $I = 10^{-12}$ A p^{-1} s^{-1}. If $\bar{R}$ is in the range 1–10 MΩ and a voltage drop of 1 V is tolerated, a data rate $N = 10^3$–10^4 particles/s^{-1} cm^{-2} is allowed for a detector of area $A = 100$ cm^2.

To experimentally investigate this point we have exposed a chamber with an anode having a 40 MΩ/square resistivity to an intense ^{55}Fe source. The source was progressively masked with an increasing number of 25 μm thick aluminum disks to reduce the input activity. Due to the continuous spectrum of ^{55}Fe

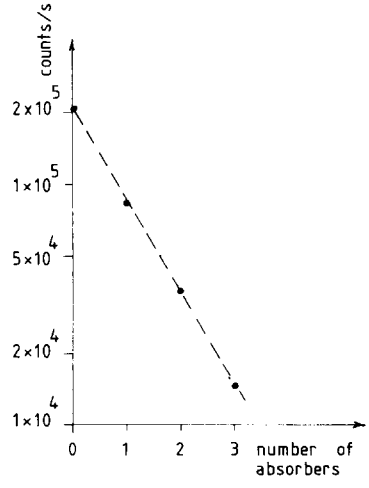

Fig. 16. The counting rate (logarithmic scale) as a function of the number of absorbers.

any gain reduction at high rate should manifest itself as a reduction of the counting rate. Fig. 16 shows the logarithm of the measured intensity as a function of the absorber thickness. No deviation from linearity was observed up to the maximum measured rate of 200 kHz.

7. Conclusions

A position sensitive parallel plate counter working at atmospheric pressure has been presented. The device is continuous, homogeneous, self-triggering and can operate at a rate $> 10^5$ particles/s. A resolution of 70 μm for both coordinates has been measured. Further tests of efficiency, time resolution and uniformity of response to minimum ionizing particles are planned for the near future.

Acknowledgements

We thank G. Favati of INFN, Pisa for the accurate mechanical work, C. Guidi of Dipartimento di Fisica dell'Università di Pisa for the assistance during the holographic measurement and G. Muratori of CERN for his hospitality during the precise machining of the epoxy plates.

References

[1] G. Hempel et al., Nucl. Instr. and Meth. 131 (1975) 445.
[2] H. Stelzer, Nucl. Instr. and Meth. 133 (1976) 409.
[3] D.V. Harrack and H.J. Specth, Nucl. Instr. and Meth. 164 (1979) 477.
[4] A. Peisert et al., IEEE Trans. Nucl. Sci. NS-31 (1984) 125.
[5] G. Battistoni et al., Nucl. Instr. and Meth. 202 (1982) 459.
[6] V. Radeka, IEEE Trans. Nucl. Sci. NS-21 (1974) 51.
[7] J. Chiba et al., Nucl. Instr. and Meth. 206 (1983) 451.
[8] W.R. Smyth, Static and Dynamic Electricity (MacGraw-Hill, New York, 1968).
[9] R. Bellazzini et al., Nucl. Instr. and Meth. 225 (1984) 145.
[10] R. Bellazzini et al., to be submitted to Nucl. Instr. Meth.